

Changes in the Tropical Cyclone Genesis Potential Index over the Western North Pacific in the SRES A2 Scenario

ZHANG Ying^{*1,2,4} (张颖), WANG Huijun^{1,2} (王会军),
SUN Jianqi^{1,2} (孙建奇), and Helge DRANGE^{1,3}

¹*Nansen-Zhu International Research Centre, Institute of Atmospheric Physics,
Chinese Academy of Sciences, Beijing 100029*

²*Climate Change Research Center, Chinese Academy of Sciences, Beijing 100029*

³*Department of Geophysics, University of Bergen, Allégaten 70, 5007 Bergen, Norway*

⁴*Graduate University of Chinese Academy of Science, Beijing 100049*

(Received 5 May 2009; revised 14 December 2009)

ABSTRACT

The Tropical Cyclone Genesis Potential Index (GPI) was employed to investigate possible impacts of global warming on tropical cyclone genesis over the western North Pacific (WNP). The outputs of 20th century climate simulation by eighteen GCMs were used to evaluate the models' ability to reproduce tropical cyclone genesis via the GPI. The GCMs were found in general to reasonably reproduce the observed spatial distribution of genesis. Some of the models also showed ability in capturing observed temporal variation. Based on the evaluation, the models (CGCM3.1-T47 and IPSL-CM4) found to perform best when reproducing both spatial and temporal features were chosen to project future GPI. Results show that both of these models project an upward trend of the GPI under the SRES A2 scenario, however the rate of increase differs between them.

Key words: Genesis Potential Index, tropical cyclone, western North Pacific, global warming, SRES A2

Citation: Zhang, Y., H. J. Wang, J. Q. Sun, and H. Drange, 2010: Changes in the Tropical Cyclone Genesis Potential Index over the western North Pacific in the SRES A2 scenario. *Adv. Atmos. Sci.*, **27**(6), 1246–1258, doi: 10.1007/s00376-010-9096-1.

1. Introduction

Tropical cyclones are a type of natural disaster, bringing violent weather such as very strong winds, heavy thunderstorms, and torrential rain. When a tropical cyclone affects China, it will usually have originated from the western North Pacific (WNP), the most active area for these phenomena. The combined effects of increasing population, increasing urbanization, and the occurrence of tropical cyclones have caused a marked rise in human and economic damage to many coastal areas. Therefore, it is of great interest and societal importance to understand how tropical cyclones are affected by climate change.

A series of studies have investigated tropical cyclone and climate change connections from an observational perspective (Chan and Liu, 2004; Emanuel, 2005; Webster et al., 2005; Fan, 2007a, b; Shepherd and Knutson, 2007; Zhou and Cui, 2008; Zhou et al., 2008; Chen, 2009). However, due to a lack of long-term and reliable data, some of the results from these analyses have proven to be controversial.

Meanwhile, many studies have used climate models to study the issue. There are two main techniques for diagnosing tropical cyclone activity in climate models. The first is to detect the location and track of individual tropical-cyclone-like vortices in a model's output (Haarsma et al., 1993; Bengtsson et

* Corresponding author: ZHANG Ying, zhangy@mail.iap.ac.cn

al., 1995; Walsh and Watterson, 1997; Camargo and Zebiak, 2002; Chauvin et al., 2006; Oouchi et al., 2006; Bengtsson et al., 2007). Usually, a series of dynamical and thermodynamical criteria are settled based on observed climatology. A simulated tropical cyclone is defined if the relevant variables exceed the threshold. For most current GCMs, the resolution is not sufficient to capture the dynamics of tropical cyclones. Therefore, in some studies, downscaling has been used as an approach to obtain reasonable results (Emanuel et al., 2008; Knutson et al., 2008). The second technique is to provide an estimate of tropical cyclone activity through large-scale environmental factors (Gray, 1979; Ryan et al., 1992; Watterson et al., 1995; Royer et al., 1998; Emanuel and Nolan, 2004). Most state-of-the-art GCMs can provide a reasonable reproduction of large-scale features of past and present climate, although they do not tend to have sufficient resolution to resolve the dynamics in the tropical cyclone. Thus far, a quantitative theory describing how large-scale features affect tropical cyclone activity is still lacking, while empirical methods have been proven to be useful approaches in some studies (Camargo et al., 2007a, b; Caron and Jones, 2008).

Gray (1979) developed an empirical tropical cyclone genesis index which can present a reasonable description of the seasonal and spatial variation of tropical cyclone genesis. However, it has been pointed out in a number of other works that the index may be not appropriate for climate change studies, since a specific threshold for thermodynamic conditions according to present climate is used (Ryan et al., 1992; Royer et al., 1998). Royer et al. (1998) improved the index by replacing the SST threshold with convective potential, which can avoid the use of parameters that might not be suitable to future climate. Caron and Jones (2008) evaluated both the original and modified index using ERA-40 data and found that both indices can obtain a reasonable global number and spatial distribution of implied tropical cyclones compared to observations. The authors also estimated the index using outputs from the World Climate Research Programme's (WCRP) Coupled Model Intercomparison Project Phase 3 (CMIP3) dataset. The modified index in a nine-model ensemble showed an increase in all the scenarios over the WNP.

Emanuel and Nolan (2004) developed another empirical index, the Genesis Potential Index (GPI), to relate tropical cyclone genesis to several large-scale environmental factors. This index has similar factors to those in Gray's index, such as wind shear and mid-tropospheric relative humidity, but with a large difference in the thermodynamic variable. The GPI uses potential intensity, which depends on the air-sea thermo-

dynamic disequilibrium and the difference between the SST and the temperature at the level of neutral buoyancy for an adiabatically lifted boundary layer parcel. Since the parameters that might be specific to present climate are avoided in developing the index, the GPI is suitable to climate change studies. Indeed, the index has been applied to reanalysis and output from climate models, with results showing that it can replicate observed seasonal variations and the location of genesis in several basins, and that there is an increase of the GPI in general over the WNP under global warming circumstance (Camargo et al., 2007a, b; Vecchi and Soden, 2007; Gualdi et al., 2008).

In this study, with a focus on the WNP (0° – 40° N, 100° – 180° E), the GPI was used to diagnose tropical cyclone genesis in WCRP-CMIP3 GCMs, and further to investigate the impact of global warming on tropical cyclone genesis. Before using the index to project future tropical cyclone genesis, the ability of the GPI itself and the GCMs to reproduce the observed spatial and temporal variation was evaluated by ERA-40 reanalysis dataset and outputs from the GCMs. The models with the best performance could then be chosen to project future GPI.

2. Method and data

The definition of the GPI is as follows:

$$\text{GPI} = |10^5 \eta|^{3/2} \left(\frac{H}{50} \right)^3 \left(\frac{V_{\text{pot}}}{70} \right)^3 \times (1 + 0.1 V_{\text{shear}})^{-2}, \quad (1)$$

where η is the absolute vorticity at 850 hPa (s^{-1}), H is the relative humidity at 600 hPa (%), V_{pot} is the potential intensity ($m s^{-1}$), and V_{shear} is the magnitude of the vertical wind shear between 850 hPa and 200 hPa ($m s^{-1}$). The technique used to calculate potential intensity was a generalization of that described in Emanuel (1995) to take into account dissipative heating (Bister and Emanuel, 1998), in addition to sea surface temperature, sea level pressure, and atmospheric temperature and mixing ratio, at various pressure levels. More detailed information about the index can be found in Emanuel and Nolan (2004) and Camargo et al. (2007a, b).

In this paper, the observed GPI was calculated from the ERA-40 reanalysis dataset (Uppala et al., 2005) and the second Hadley Centre Sea Surface Temperature (HadSST2) dataset (Rayner et al., 2006). The observed cyclone genesis events, taken from the Joint Typhoon Warning Center (JTWC) best track dataset, were used to estimate the GPI's ability at de-

Table 1. Selected model features. Partly extracted from Randall et al. (2007) (Table 8.1).

Model ID, Year	Atmosphere Top, Resolution, References	Ocean Resolution, Z Coordinate, Top BC References	Coupling Flux Adjustments, References
BCCR-BCM2.0, 2005	top=10 hPa, T63 ($1.9^\circ \times 1.9^\circ$) L31, (Déqué et al., 1994)	$(0.5^\circ - 1.5^\circ) \times 1.5^\circ$ L35, density, free surface, (Bleck et al., 1992)	no adjustments, (Furevik et al., 2003)
CCSM3, 2005	top=2.2 hPa, T85 ($1.4^\circ \times 1.4^\circ$) L26, (Collins et al., 2004)	$(0.3^\circ - 1^\circ) \times 1^\circ$ L40, depth, free surface, (Smith and Gent, 2002)	no adjustments, (Collins et al., 2006)
CGCM3.1(T47), 2005	top=1 hPa, T47 ($\sim 2.8^\circ \times 2.8^\circ$) L31, (McFarlane et al., 1992; Flato, 2005)	$1.9^\circ \times 1.9^\circ$ L29, depth, rigid lid, (Pacanowski et al., 1993)	heat, freshwater, (Flato, 2005)
CNRM-CM3, 2004	top=0.05 hPa, T63 ($\sim 1.9^\circ \times 1.9^\circ$) L45, (Déqué et al., 1994)	$(0.5^\circ - 2^\circ) \times 2^\circ$ L31, depth, rigid lid, (Madec et al., 1998)	no adjustments, (Terray et al., 1998)
CSIRO-MK3.0, 2001	top=4.5 hPa, T63 ($\sim 1.9^\circ \times 1.9^\circ$) L18, (Gordon et al., 2002)	$(0.8^\circ \times 1.9^\circ)$ L31, depth, rigid lid, (Gordon et al., 2002)	no adjustments, (Gordon et al., 2002)
CSIRO-MK3.5, 2006	top=4.5 hPa, T63 ($\sim 1.9^\circ \times 1.9^\circ$) L18, (Gordon et al., 2002)	$(0.8^\circ \times 1.9^\circ)$ L31, depth, rigid lid, (Gordon et al., 2002)	no adjustments, (Gordon et al., 2002)
ECHAM5/MPI-OM, 2005	top=10 hPa, T63 ($\sim 1.9^\circ \times 1.9^\circ$) L31, (Roeckner et al., 2003)	$(1.5^\circ \times 1.5^\circ)$ L40, depth, free surface, (Marsland et al., 2003)	no adjustments, (Jungclaus et al., 2005)
GFDL-CM2.0, 2005	top=3 hPa, $2.0^\circ \times 2.5^\circ$ L24, (GFDL GAMDT, 2004)	$(0.3^\circ - 1.0^\circ) \times 1.0^\circ$, depth, free surface, (Gnanadesikan et al., 2004)	no adjustments, (Delworth et al., 2006)
GFDL-CM2.1, 2005	top=3 hPa, $(2.0^\circ \times 2.5^\circ)$ L24, with semi-Lagrangian transports (GFDL GAMDT, 2004)	$(0.3^\circ - 1.0^\circ) \times 1.0^\circ$, depth, free surface,	no adjustments, (Delworth et al., 2006)
GISS-ER, 2004	top=0.1 hPa, $(4^\circ \times 5^\circ)$ L20, (Schmidt et al., 2006)	$(4^\circ \times 5^\circ)$ L13, mass/area, free surface, (Russell et al., 1995)	no adjustments, (Schmidt et al., 2006)
INGV-SXG, 2005	top=10 hPa, T106 ($\sim 1.125^\circ \times 1.125^\circ$) L19, (Roeckner et al., 1996)	$(0.5^\circ - 2^\circ) \times 2^\circ$ L31, depth, free surface, (Madec et al., 1999)	no adjustment, (Valcke et al., 2000)
INM-CM3.0, 2004	top=10 hPa, $(4^\circ \times 5^\circ)$ L21, (Alxeev et al., 1998; Galin et al., 2003)	$(2^\circ \times 2.5^\circ)$ L33, sigma, rigid lid, (Diansky et al., 2002)	regional freshwater, (Diansky and Volodin, 2002; Volodin and Diansky, 2004)
IPSL-CM4, 2005	top=4 hPa, $(2.5^\circ \times 3.75^\circ)$ L19, (Hourdin et al., 2006)	$(2^\circ \times 2^\circ)$ L31, depth, free surface, (Madec et al., 1998)	no adjustments, (Marti et al., 2005)
MIROC3.2(medres), 2004	Top=30 km, T42 ($\sim 2.8^\circ \times 2.8^\circ$) L20, (K-1 Model Developers, 2004)	$(0.5^\circ - 1.4^\circ) \times 1.4^\circ$ L43, sigma/depth, free surface (K-1 Model Developers, 2004)	no adjustments, (K-1 Model Developers, 2004)
MRI-CGCM2.3.2, 2003	top=0.4 hPa, T42 ($\sim 2.8^\circ \times 2.8^\circ$) L30, (Shibata et al., 1999)	$(0.5^\circ - 2.0^\circ) \times 2.5^\circ$ L23, depth, rigid lid, (Yukimoto et al., 2001)	heat, freshwater, momentum ($12^\circ\text{S} - 12^\circ\text{N}$) (Yukimoto et al., 2001; Yukimoto and Noda, 2003)

Table 1. Continued.

Model ID, Vintage	Atmosphere Top Resolution References	Ocean Resolution Z Coord, Top BC References	Coupling Flux Adjustments References
PCM, 1998	top = 2.2 hPa, T42 ($\sim 2.8^\circ \times 2.8^\circ$) L26, (Kiehl et al., 1998)	$0.5^\circ - 0.7^\circ \times 1.1^\circ$ L40, depth, free surface, (Maltrud et al., 1998)	no adjustments, (Washington et al., 2000)
UKMO-HadCM3, 1997	top=5 hPa, $2.5^\circ \times 3.75^\circ$ L19, (Pope et al., 2000)	$1.25^\circ \times 1.25^\circ$ L20, depth, rigid lid, (Gordon et al., 2000)	no adjustments, (Gordon et al., 2000)
UKMO-HadGEM1, 2004	top=39.2 km, $\sim 1.3^\circ \times 1.9^\circ$ L38, (Martin et al., 2004)	$(0.3^\circ - 1.0^\circ) \times 1.0^\circ$ L40, depth, free surface, (Roberts, 2004)	no adjustments, (Johns et al., 2006)

scribing the spatial and temporal features of cyclone genesis.

The output of “20th Century Climate in Coupled Models” (20C3M), a pilot project of CMIP, was used to estimate the ability of the GCMs to reproduce tropical cyclone genesis via the GPI. This project collects data from 20th century simulations from coupled ocean–atmosphere GCMs, driven by prescribed forcings such as increases in the atmospheric concentration of anthropogenic greenhouse gases and aerosols. The levels of these forcings are based on historical observations or reconstructions. The simulation started typically in the late 19th century and finished at the end of 20th century.

Forcings in the experiment employed in this study, as future climate realization under a background of global warming, were based on the A2 storyline in the IPCC’s Special Report on Emissions Scenarios (SRES) (Nakicenovic et al., 2000). Eighteen models were used: BCCR-BCM2.0, CCSM3, CGCM3.1-T47, CNRM-CM3, CSIRO-Mk3.0, CSIRO-Mk3.5, GFDL-CM2.0, GFDL-CM2.1, GISS-ER, INGV-SXG, INM-CM3.0, IPSL-CM4, MIROC3.2-M, MPI, MRI-CGCM2.3.2,

PCM, UKMO-HadCM3, and UKMO_HadGEM1. Table 1 lists the features of all these selected models. All the outputs of the models were taken from the WCRP-CMIP3 multi-model dataset (Meehl et al., 2007), and more detailed information about the models and experiments are available from http://www-pcmdi.llnl.gov/ipcc/about_ipcc.php. Only one realization was selected from each of the model outputs.

3. The GPI in the ERA-40 reanalysis

In this section, we describe how the JTWC best track data was used to validate the performance of the GPI in describing tropical cyclone genesis over the WNP. Different from previous studies which have used NCEP–NCAR reanalysis data (Camargo et al., 2007a, b), here, the ERA-40 reanalysis dataset was employed. Bearing in mind the quality of the observation dataset before the 1970s (Emanuel, 2005), and that the 20C3M simulations in some models end at 1999, the evaluation analysis period in this study was confined to 1970–1999.

The climatology of observed cyclone genesis and

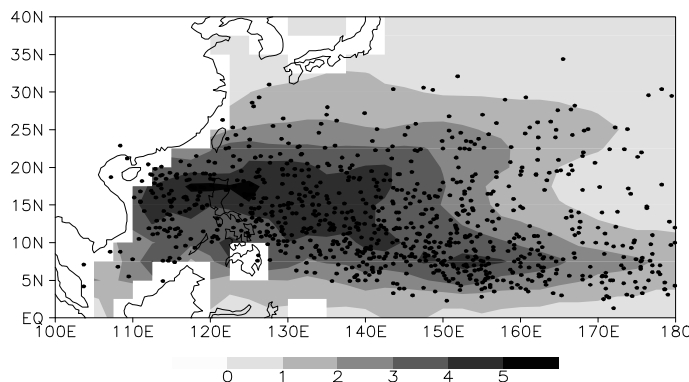


Fig. 1. Observed GPI climatology estimated by ERA-40 (shaded) and tropical cyclone genesis events (black dots) during 1970–1999.

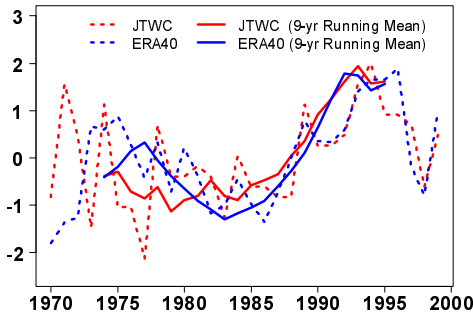


Fig. 2. Interannual and interdecadal (9-yr running mean) variation of the GPI and tropical cyclone genesis in the JTWC best track dataset. All time series are normalized. The GPI was averaged over (0° – 40° N, 100° – 180° E).

the GPI over the WNP is displayed in Fig. 1. The climatological GPI was the composite of monthly mean GPI calculated from reanalysis data. The results show most of the tropical cyclones occurring over a zone between 5° – 30° N, with a maximum centre over the region 10° – 20° N, 110° – 160° E. The distribution of the GPI shows a similar spatial pattern, with a relatively high GPI located over the middle of the tropical WNP, indicating that GPI can depict well the spatial distribution of observed tropical cyclone occurrence.

Figure 2 displays the interannual and interdecadal variation (9-yr running mean) of observed tropical cyclone genesis and area mean GPI over the WNP. As can be seen, the interannual variability of the GPI and observed tropical cyclone genesis show similar features. The correlation coefficient between them is 0.45, which is significant at the 95% confidence level. On the interdecadal timescale, the GPI exhibits a better performance, with the correlation coefficient up to 0.90. This indicates that the GPI can also reasonably infer the temporal characteristics of tropical cyclone genesis.

Therefore, in the following analysis, the GPI was chosen as a proxy index to investigate the ability of the climate models to simulate the WNP cyclone genesis, and further to project changes in WNP cyclone genesis under a background of global warming.

4. The GPI in the 20C3M experiment

Confidence in the projection of future climate by models depends mainly on their ability to reproduce past and present climate. Therefore, the outputs of 20C3M simulations by eighteen GCMs from the WCRP-CMIP3 multi-model dataset were used to evaluate the performance of the models at describing present cyclone genesis. Since the resolution of the models are not identical, the model fields were inter-

polated to the same resolution as the ERA-40 dataset.

Figure 3 shows the climatology of the GPI in all eighteen GCMs during 1970–1999. For the spatial structure, most of the models could generally reproduce the distribution of tropical cyclone genesis over the WNP, as shown in Fig. 1. However, there are systematic biases in some of the models. For example, the maximum center in CNRM-CM3 and PCM shows a northward shift, and in INM-CM3 an eastward shift, as compared to the most active genesis area shown in Fig. 1. In addition, all of the models more or less underestimated the GPI compared to that estimated from the ERA-40 reanalysis data, except for the MPI model.

Interannual variation of the GPI in the eighteen GCMs is shown in Fig. 4. It can be seen that most of the models were poor at reproducing interannual variation of tropical cyclone genesis. Only CGCM3.1-T47 and IPSL-CM4 obtained a reasonable result. The year-to-year variation of the GPI in these two models was significantly correlated to that in observed data at the 95% confidence level. As shown in Fig. 5, some models showed much better performance on the interdecadal timescale, such as CGCM3.1-T47, CSIRO-Mk3.5, GFDL-CM2.1, INGV-SXG, IPSL-CM4, MRI-CGCM2.3.2, and UKMO-HadGEM1. The interdecadal variation in these models and that in the observed data was significantly correlated at the 95% confidence level. Among them, CGCM3.1-T47 and IPSL-CM4 showed the best performance. The interdecadal variation in these two models fitted observed results very well, with correlation coefficients of 0.91 and 0.88, respectively.

Taking into account spatial distribution, and interannual and interdecadal variation, two of the eighteen models, CGCM3.1-T47 and IPSL-CM4, showed the best performance. In order to reduce the uncertainty in projection, we therefore chose these two models to project future GPI under SRES A2.

5. The GPI in the SRES A2 experiment

Figure 6 shows projected changes in the GPI during the 21st century in the SRES A2 experiment, relative to the 1980–1999 climatology in the 20C3M experiment. The results suggest that there might be a higher GPI over most of the WNP in the middle period of the 21st century (2041–2060) in CGCM3.1-T47. The largest increase would be over the area 10° – 20° N, with the rate of increase being above 15%. The change projected to occur in the late 21st century (2081–2100) is similar to that in middle period of the 21st century, but with a larger increment. The change projected by IPSL-CM4 shows similar features. However, a de-

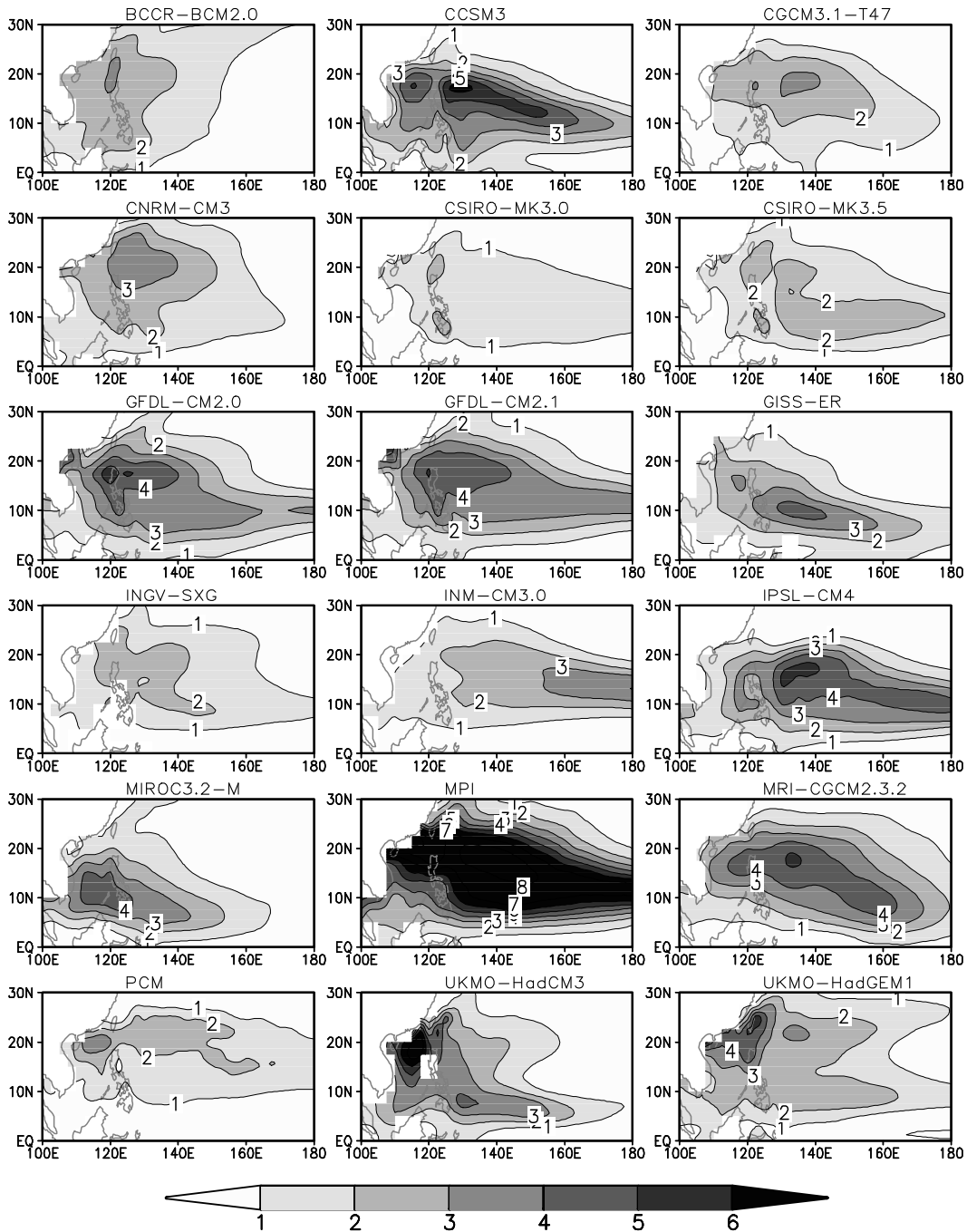


Fig. 3. Climatology of the GPI in 18 GCMs during 1970–1999 in the 20C3M simulation.

crease is found over the area south of 10°N , east of 135°E . The decrease is relatively weak and locates in the area south of 5°N in CGCM3.1-T47. These results indicate that there might be more tropical cyclones generated over the area north of 10°N , as inferred by the GPI under a background of global warming. However, there is relatively large uncertainty in projecting changes in the GPI over the area south of 10°N .

Interdecadal and interannual variations of the GPI

in the CGCM3.1-T47 and IPSL_CM4 models are displayed in Fig. 7. The bold line indicates the 9-yr running mean. The results show an upward trend in both models, but the rate of increase differs between them. In CGCM3.1-T47, the rate of increase during 2041–2060 (2081–2100) is projected to be 13% (20%), compared to 1980–1999 climatology. Meanwhile, in IPSL_CM4, the rate of increase during 2041–2060 (2081–2100) is predicted to be 7% (9%). These results indi-

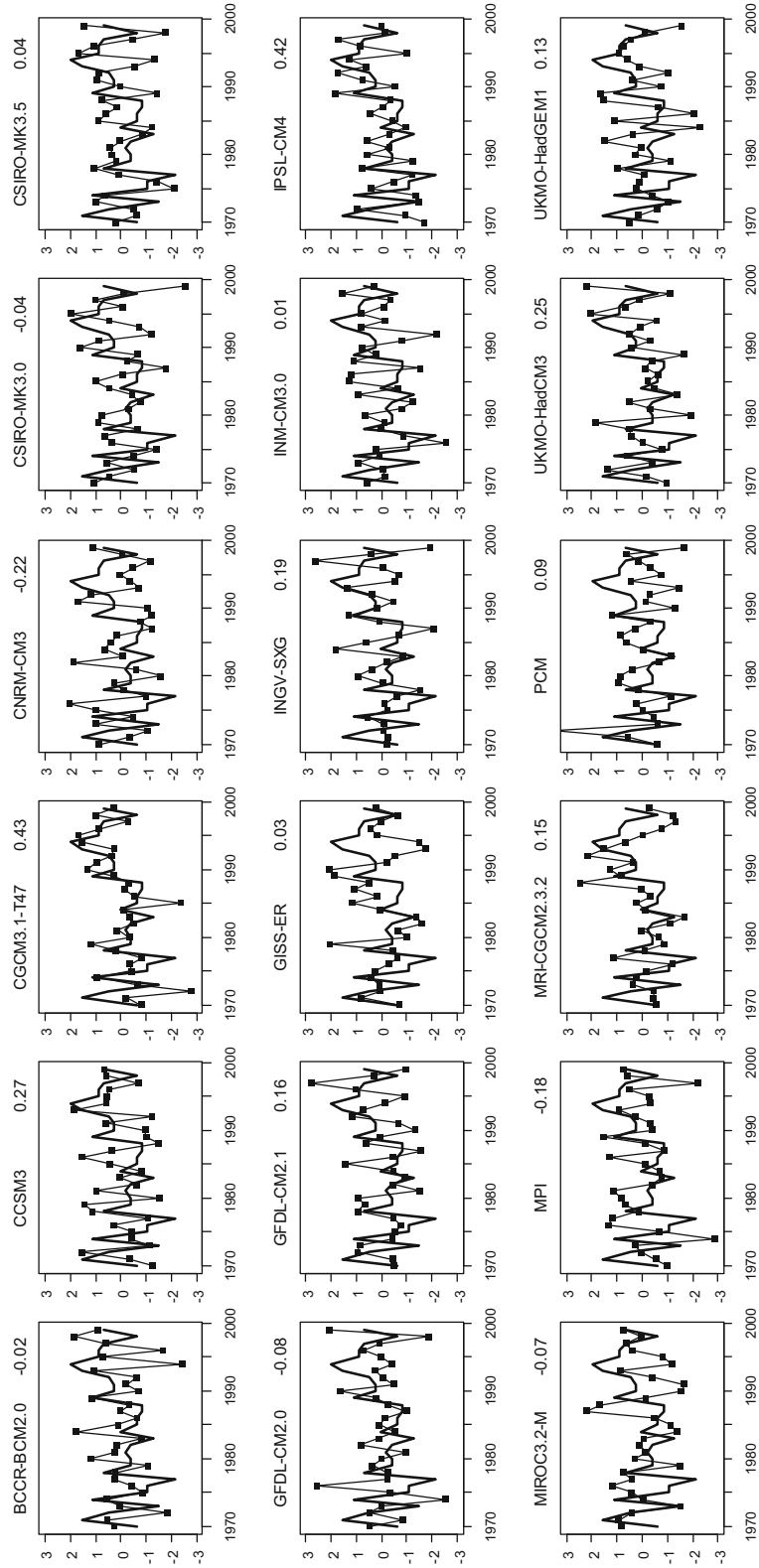


Fig. 4. Interannual variation of the GPI during 1970–1999 in the 20C3M simulation. The lines with squares indicate outputs from the models, and bold lines show interannual variation of tropical cyclone genesis from the JTWC best track dataset. All time series are normalized. The number on top of each plot is the correlation of two time series. The GPI is averaged over $(0^{\circ}$ – 40° N, 100° – 180° E).

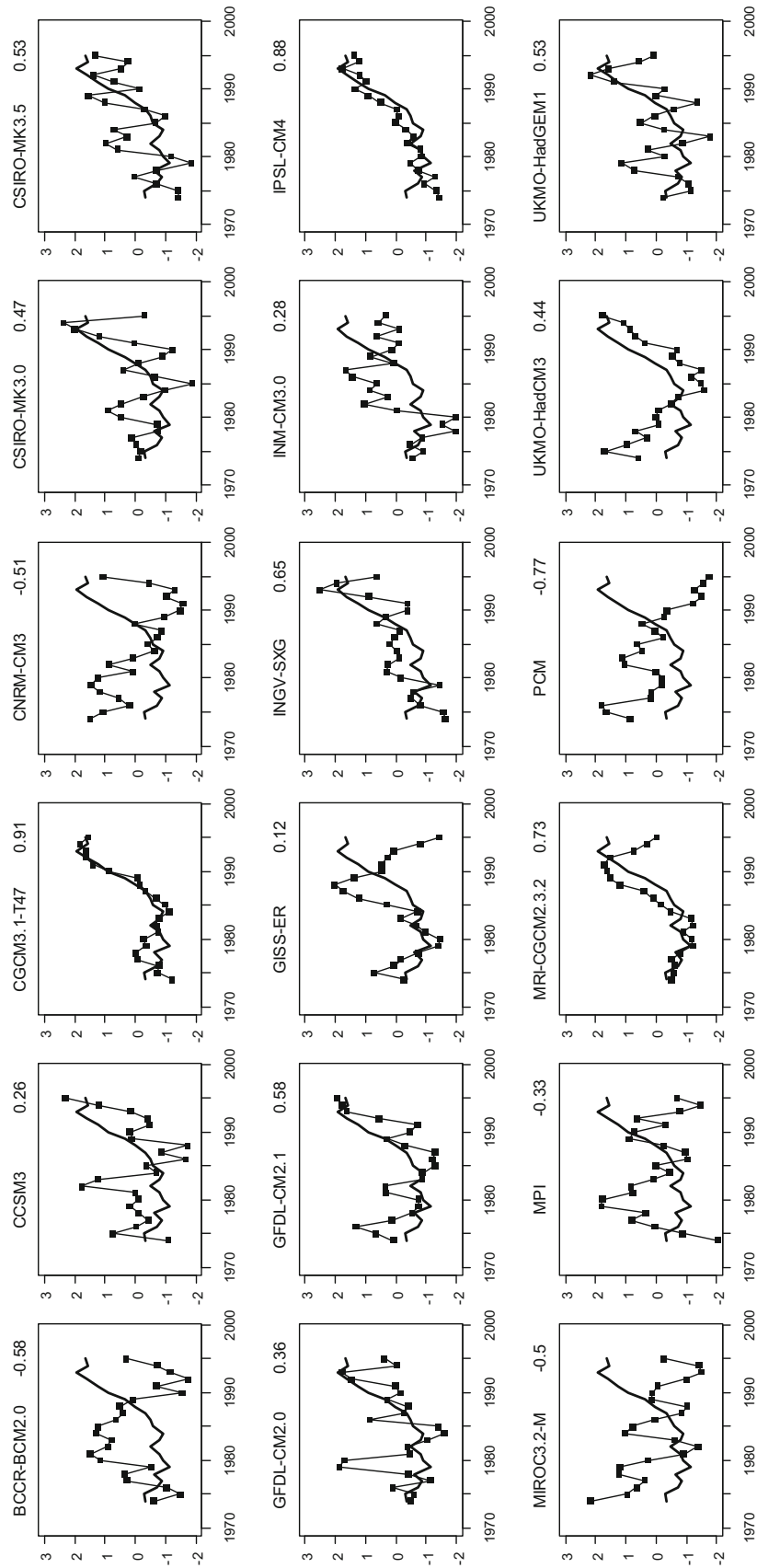


Fig. 5. Same as Fig. 4, but for interdecadal variation.

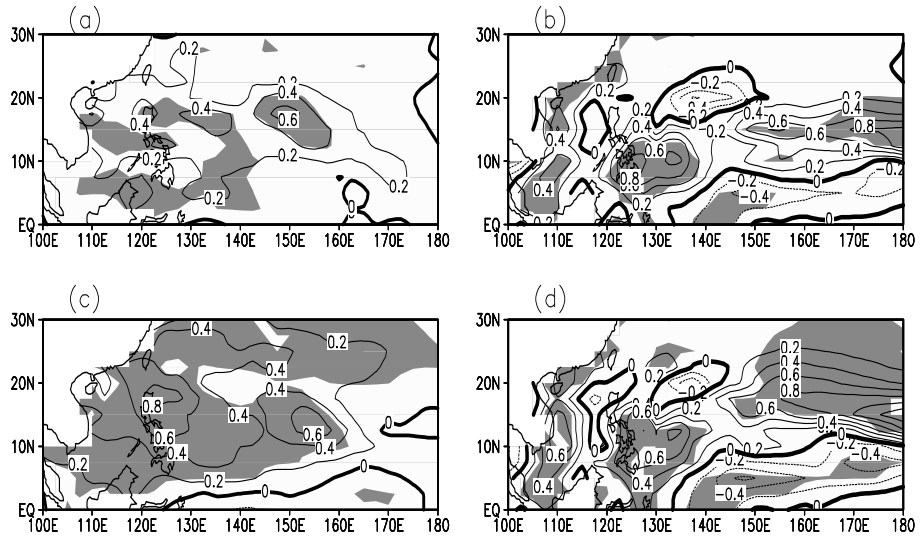


Fig. 6. Spatial distribution of change of the GPI in SRES A2 simulation: (a) Change in 2041–2060 climatology compared to 1980–1999 climatology in the 20C3M experiment in CGCM3.1-T47; (c) change in 2081–2100 climatology; (b) and (d) change in the GPI in IPSL-CM4. Shading denotes changes statistically significant at the 95% confidence level.

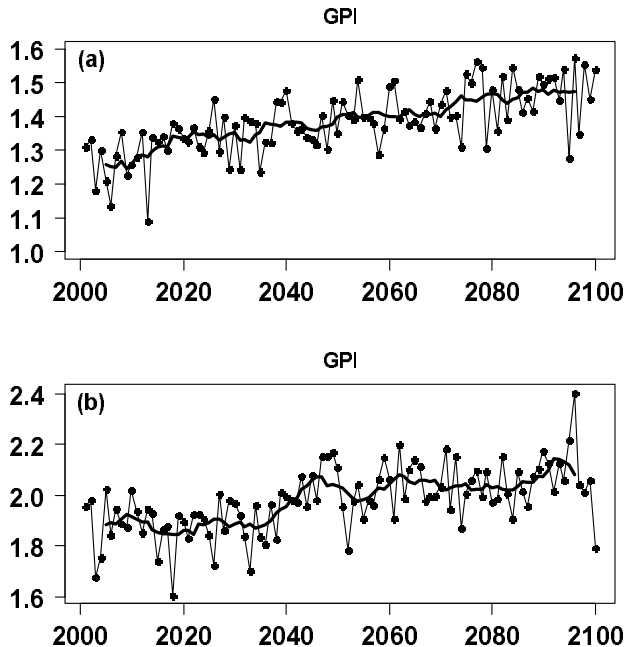


Fig. 7. Temporal variation of the GPI index during the 21st century in SRES A2 simulation. (a) and (b) show interannual and interdecadal variation of the GPI in CGCM3.1-T47 and IPSL-CM4, respectively. Bold lines indicate interdecadal variation. The GPI is averaged over (0°–40°N, 100°–180°E).

cate that, as inferred by the GPI, tropical cyclone genesis could become more frequent over the WNP on the

whole, but there is large uncertainty in projecting the rate of increase.

Also analyzed were the possible changes in the four components of the GPI. Figures 8 and 9 show the annual mean of the four components [absolute vorticity parameter, $|10^5 \eta|^{3/2}$; relative humidity parameter, $(H/50)^3$; potential intensity parameter, $(V_{\text{pot}}/70)^3$; and wind shear parameter, $(1 + 0.1 V_{\text{shear}})^{-2}$] averaged over the area (0° – 30° N, 100° – 180° E) during the 21st century in CGCM3.1-T47 and IPSL-CM4. The percentage change in the relative humidity parameter is projected to be 30% and 8% in the models at the end of the 21st century, while changes in the other parameters are not predicted to be larger than 5%. Therefore, through the above analysis, changes in the GPI are projected to be mainly attributable to changes in relative humidity, as compared to the other three factors.

6. Summary and discussion

In this study, an empirical index, the GPI, was used as a proxy index to project future tropical cyclone genesis by GCMs. Estimation of the GPI from ERA-40 reanalysis data showed that the GPI can capture the main characteristics of spatial distribution and temporal variation of genesis, as observed in the JTWC best track dataset, indicating that the index could be used to infer tropical cyclone genesis over the WNP. The GPI estimated by the output of the 20C3M simulation showed that the GCMs could generally reproduce

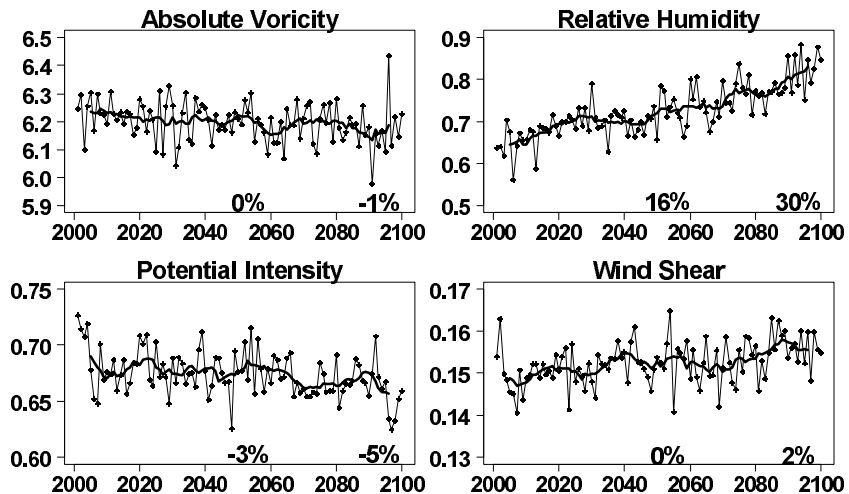


Fig. 8. Temporal variation of absolute vorticity parameter ($|10^5 \eta|^{3/2}$), relative humidity parameter $\left[\left(\frac{H}{50}\right)^3\right]$, potential intensity parameter $\left[\left(\frac{V_{pot}}{70}\right)^3\right]$, and wind shear parameter $\left[(1 + 0.1V_{shear})^{-2}\right]$ in the CGCM3.1-T47 model. Numbers at the bottom of each plot indicate the rate of change during 2040–2059 and 2080–2099, compared to 1980–1999 climatology. All variables are averaged over $(0^\circ\text{--}30^\circ\text{N}, 100^\circ\text{--}180^\circ\text{E})$.

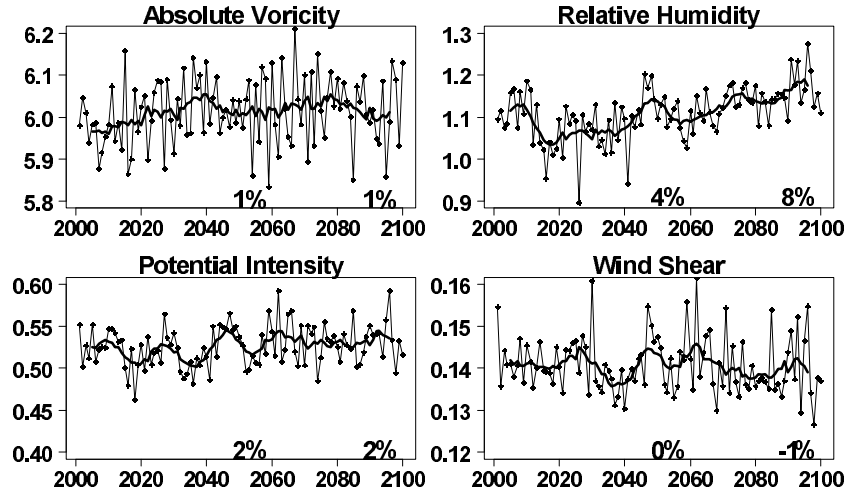


Fig. 9. Same as Fig. 8 but for the IPSL-CM4 model.

the spatial pattern of genesis. Some of the models also showed an ability to capture the temporal variation in observed cyclone genesis. Taking into account the ability of the climate models to simulate both spatial and temporal features, CGCM3.1-T47 and IPSL-CM4, which demonstrated the best performance, were chosen to project changes in cyclone genesis over the WNP under SRES A2. Both of the models predicted an upward trend of the WNP GPI during the 21st century, indicating that there might be more tropical cyclones generated over the WNP in the future. However, the rate of increase in the two models differed,

with CGCM3.1-T47 showing a rate of increase of up to 20% and IPSL-CM4 showing a rate of increase of up to 9% in the late 21st century. This means that there is larger uncertainty in projecting the rate of increase than the sign of change.

The positive trend in the GPI is similar to the work of Caron and Jones (2008). They found that the CYGP (convective yearly genesis potential) index has a positive trend over the WNP under a global warming scenario. The rate of increase in a nine-model ensemble was found to be up to 22% in the late 21st century under SRES A2. Vecchi and Soden (2007) showed

changes in several factors, which were also used in the present study, under SRES A1B by 18 WCRP-CMIP3 GCMs. The multi-model ensemble mean showed that there will be hurricane-favorable conditions over the WNP.

However, Gualdi et al. (2008) used a different approach, detecting simulated tropical cyclones in a high resolution GCM and finding a reduction in tropical cyclones over the WNP when the greenhouse gas concentration doubled and quadrupled. They also calculated the GPI using the same model output and found that the GPI showed some increases over the WNP. Clearly, the results derived from the two approaches do not agree well with each other. As shown in Figs. 8 and 9, relative humidity makes a big contribution to the increase of the GPI over the WNP. However, this factor was not directly employed in the tropical cyclone detecting method in the analysis of Gualdi et al. (2008). This could be one of the potential reasons for the inconsistency in the results, indicating there remains considerable uncertainty in projecting future tropical cyclone activity. This issue needs further exploration.

Acknowledgements. The authors acknowledge the modeling groups, the Program for Climate Model Diagnosis and Intercomparison (PCMDI), and the WCRP's Working Group on Coupled Modelling (WGCM), for their roles in making available the WCRP CMIP3 multi-model dataset. Support for this dataset was provided by the Office of Science, US Department of Energy. The authors also appreciate the comments of the two anonymous reviewers. This research was jointly supported by the Chinese Academy of Sciences under (Grant Nos. KZCX2-YW-Q1-02 and KZCX2-YW-Q11-05), the Major State Basic Research Development Program of China (973 Program) (Grant No. 2009CB421407), and the National Natural Science Foundation of China (Grant Nos. 40631005, 40775049, and 40805029). This research also received financial support from the Nansen Scientific Society for the first author's visiting research in the Nansen Environmental and Remote Sensing Center.

REFERENCES

- Bengtsson, L., M. Botzet, and M. Esch, 1995: Hurricane-type vortices in a general-circulation model. *Tellus (A)*, **47**(2), 175–196.
- Bengtsson, L., K. I. Hodges, M. Esch, N. Keenlyside, J. J. Luo, and T. Yamagata, 2007: How may tropical cyclones change in a warmer climate? *Tellus (A)*, **59**(4), 539–561.
- Bister, M., and K. Emanuel, 1998: Dissipative heating and hurricane intensity. *Meteor. Atmos. Phys.*, **52**, 233–240.
- Bleck, R., C. Rooth, D. Hu, and L.T. Smith, 1992: Salinity-driven thermocline transients in a wind- and thermohaline-forced isopycnic coordinate model of the North Atlantic. *J. Phys. Oceanogr.*, **22**, 1486–1505.
- Camargo, S. J., and S. E. Zebiak, 2002: Improving the detection and tracking of tropical cyclones in atmospheric general circulation models. *Wea. Forecasting*, **17**(6), 1152–1162.
- Camargo, S. J., K. A. Emanuel, and A. H. Sobel, 2007a: Use of a genesis potential index to diagnose ENSO effects on tropical cyclone genesis. *J. Climate*, **20**(19), 4819–4834.
- Camargo, S. J., A. H. Sobel, A. G. Barnston, and K. A. Emanuel, 2007b: Tropical cyclone genesis potential index in climate models. *Tellus(A)*, **59**(4), 428–443.
- Caron, L. P., and C. G. Jones, 2008: Analysing present, past and future tropical cyclone activity as inferred from an ensemble of coupled global climate models. *Tellus(A)*, **60**, 80–96.
- Chan, J. C. L., and K. S. Liu, 2004: Global warming and western North Pacific typhoon activity from an observational perspective. *J. Climate*, **17**(23), 4590–4602.
- Chauvin, F., J. F. Royer, and M. Deque, 2006: Response of hurricane-type vortices to global warming as simulated by ARPEGE-Climat at high resolution. *Climate Dyn.*, **27**(4), 377–399.
- Chen, G. H., 2009: Interdecadal variation of tropical cyclone activity in association with summer monsoon, sea surface temperature over the western North Pacific. *Chinese Science Bulletin*, **54**(8), 14417–1421.
- Collins, W. D., P. J. Rasch, B. A. Boville, J. J. Hack, J. R. McCaa, D. L. Williamson, J. T. Kiehl, and B. Briegleb, 2004: Description of the NCAR Community Atmosphere Model (CAM3.0). Technical Note TN-464+STR, National Center for Atmospheric Research, Boulder, CO, 226pp. [Available online from <http://www.cesm.ucar.edu/models/atm-cam/docs/description/description.pdf>]
- Collins, W. D., and Coauthors, 2006: The Community Climate System Model: CCSM3. *J. Climate*, **19**, 2122–2143.
- Delworth, T. and Coauthors, 2006: GFDL's CM2 global coupled climate models—Part 1: Formulation and simulation characteristics. *J. Climate*, **19**, 643–674.
- Déqué, M., C. Dreveton, A. Braun, and D. Cariolle, 1994: The ARPEGE/IFS atmosphere model: A contribution to the French community climate modeling. *Climate Dyn.*, **10**, 249–266.
- Diansky, N. A., and E. M. Volodin, 2002: Simulation of the present-day climate with a coupled atmosphere-ocean general circulation model. *Izv. Atmos. Ocean. Phys.*, **38**, 732–747. (English translation).
- Emanuel, K. A., 1995: Sensitivity of tropical cyclones to surface exchange coefficients and a revised steady-state model incorporating eye dynamics. *J. Atmos. Sci.*, **52**(22), 3969–3976.
- Emanuel, K., 2005: Increasing destructiveness of tropical

- cyclones over the past 30 years. *Nature*, **436**(7051), 686–688.
- Emanuel, K. A., and D. S. Nolan, 2004: Tropical cyclone activity and global climate. *Bull. Amer. Metror. Soc.*, **85**(5), 666–667.
- Emanuel, K., R. Sundararajan, and J. Williams, 2008: Hurricanes and global warming: results from downscaling IPCC AR4 simulations. *Bull. Amer. Meteor. Soc.*, **89**(3), 347–367.
- Fan, K., 2007a: New predictos and a new prediction model for the typhoon frequency over western North Pacific. *Science in China(D)*, **50**(9), 1417–1423.
- Fan, K., 2007b: North Pacific sea ice cover, a predictor for the western North Pacific typhoon frequency? *Science in China(D)*, **50**(8), 1251–1257.
- Flato, G. M., 2005: The Third Generation Coupled Global Climate Model (CGCM3) [Available online from <http://www.cccma.bc.ec.gc.ca/models/cgcm3.shtml>.]
- Furevik, T., M. Bentsen, H. Drange, I. K. T. Kindem, N. G. Kvamstø, and A. Sorteberg, 2003: Description and evaluation of the Bergen climate model: ARPEGE coupled with MICOM. *Climate Dyn.*, **21**, 27–51.
- Galin, V. Ya., E. M. Volodin, and S. P. Smyshliaev, 2003: Atmospheric general circulation model of INM RAS with ozone dynamics. *Russian Meteorology and Hydrology*, **5**, 13–22.
- GFDL GAMDT (The GFDL Global Atmospheric Model Development Team), 2004: The new GFDL global atmosphere and land model AM2-LM2: Evaluation with prescribed SST simulations. *J. Climate*, **17**, 4641–4673.
- Gnanadesikan, A., and Coauthors, 2004: GFDL's CM2 global coupled climate models—Part 2: The baseline ocean simulation. *J. Climate*, **19**, 675–697.
- Gordon, C., C. Cooper, C. A. Senior, H. Banks, J. M. Gregory, T. C. Johns, J. F. B. Mitchell, and R. A. Wood, 2000: The simulation of SST, sea ice extents and ocean heat transports in a version of the Hadley Centre coupled model without flux adjustments. *Climate Dyn.*, **16**, 147–168.
- Gordon, H. B., and Coauthors, 2002: The CSIRO Mk3 Climate System Model. CSIRO Atmospheric Research Technical Paper No. 60, Commonwealth Scientific and Industrial Research Organisation Atmospheric Research, Aspendale, Victoria, Australia, 130pp.
- Gray, W. M., 1979: Hurricanes: Their formation, structure, and likely role in the tropical circulation. *Meteorology over the Tropical Oceans*, Shaw, Ed., Royal Meteorological Society, 155–218.
- Gualdi, S., E. Scoccimarro, and A. Navarra, 2008: Changes in Tropical Cyclone Activity due to Global Warming: Results from a High-Resolution Coupled General Circulation Model. *J. Climate*, **21**(20), 5204–5228.
- Haarsma, R. J., J. F. B. Mitchell, and C. A. Senior, 1993: Tropical disturbances in a gcm. *Climate Dyn.*, **8**(5), 247–257.
- Houardin, F., and Coauthors, 2006: The LMDZ4 general circulation model: Climate performance and sensitivity to parameterized physics with emphasis on tropical convection. *Climate Dyn.*, **27**, 787–813.
- Johns, T. C., and Coauthors, 2006: The new Hadley Centre climate model HadGEM1: Evaluation of coupled simulations. *J. Climate*, **19**, 1327–1353.
- Jungclaus, J. H., and Coauthors, 2006: Ocean circulation and tropical variability in the coupled model ECHAM5/MPI-OM. *J. Climate*, **19**, 3952–3972.
- K-1 Model Developers, 2004: K-1 Coupled Model (MIROC) Description. K-1 Technical Report 1. H. Hasumi, and S. Emori, Eds., Center for Climate System Research, University of Tokyo, Tokyo, Japan, 34 pp.
- Kiehl, J. T., and Coauthors, 1998: The National Center for Atmospheric Research Community Climate Model: CCM3. *J. Climate*, **11**, 1131–1149.
- Knutson, T. R., J. J. Sirutis, S. T. Garner, G. A. Vecchi, and I. M. Held, 2008: Simulated reduction in Atlantic hurricane frequency under twenty-first-century warming conditions. *Nature Geoscience*, **1**, 359–364.
- Madec, G., P. Delecluse, M. Imbard, and C. Lévy, 1998: OPA Version 8.1 Ocean General Circulation Model Reference Manual. Notes du Pôle de Modélisation No. 11, Institut Pierre-Simon Laplace, Paris, 91pp.
- Maltrud, M. E., R. D. Smith, A. J. Semtner, and R. C. Malone, 1998: Global eddy-resolving ocean simulations driven by 1985–1995 atmospheric winds. *J. Geophys. Res.*, **103**, 30825–30853.
- Marsland, S. J., H. Haak, J. H. Jungclaus, M. Latif, and F. Roeske, 2003: The Max-Planck-Institute global ocean/sea ice model with orthogonal curvilinear coordinates. *Ocean Modelling*, **5**, 91–127.
- Marti, O., and Coauthors, 2005: The New IPSL Climate System Model: IPSL-CM4. Note du Pôle de Modélisation No. 26, Institut Pierre Simon Laplace des Sciences de l'Environnement Global, Paris.
- Martin, G. M., and Coauthrs, 2004: Evaluation of the Atmospheric Performance of HadGAM/GEM1. Hadley Centre Technical Note No. 54, Hadley Centre for Climate Prediction and Research/Met Office, Exeter, UK.
- McFarlane, N. A., G. J. Boer, J.-P. Blanchet, and M. Lazare, 1992: The Canadian Climate Centre second-generation general circulation model and its equilibrium climate. *J. Climate*, **5**, 1013–1044.
- Meehl, G. A., C. Covey, T. Delworth, M. Latif, B. Mcavaney, J. F. B. Mitchell, R. J. Stouffer, and K. E. Taylor, 2007: The WCRP CMIP3 multimodel dataset: A new era in climate change research. *Bull. Amer. Meteor. Soc.*, **88**, 1383–1394.
- Nakicenovic, N., and Coauthors, 2000: *IPCC Special Report on Emissions Scenarios*. Cambridge University Press, Cambridge, 599pp.
- Oouchi, K., J. Yoshimura, H. Yoshimura, R. Mizuta, S. Kusunoki, and A. Noda, 2006: Tropical cyclone climatology in a global-warming climate as simulated in

- a 20 km-mesh global atmospheric model: Frequency and wind intensity analyses. *J. Meteor. Soc. Japan*, **84**(2), 259–276.
- Pacanowski, R. C., K. Dixon, and A. Rosati, 1993: The GFDL Modular Ocean Model Users Guide, Version 1.0. GFDL Ocean Group Technical Report No. 2, Geophysical Fluid Dynamics Laboratory, Princeton, NJ.
- Pope, V. D., M. L. Gallani, P. R. Rountree, and R. A. Stratton, 2000: The impact of new physical parameterizations in the Hadley Centre climate model: HadAM3. *Climate Dyn.*, **16**, 123–146.
- Randall, D. A., and Coauthors, 2007: *Climate Models and Their Evaluation. Climate Change 2007: The Physical Science Basis, Contribution of Working Group I to the Fourth Assessment Report of the Intergovernmental Panel on Climate Change*, Solomon et al., Eds., Cambridge University Press, Cambridge, United Kingdom and New York, NY, USA, 589–662.
- Rayner, N. A., P. Brohan, D. E. Parker, C. K. Folland, J. J. Kennedy, M. Vanicek, T. J. Ansell, and S. F. B. Tett, 2006: Improved analyses of changes and uncertainties in sea surface temperature measured in situ since the mid-nineteenth century: The HadSST2 dataset. *J. Climate*, **19**(3), 446–469.
- Roberts, M. J., 2004: The Ocean Component of HadGEM1. GMR Report Annex IV.D.3, Met Office, Exeter, UK.
- Roeckner, E., and Coauthors, 1996: The Atmospheric General Circulation Model ECHAM4: Model Description and Simulation of Present-Day Climate. MPI Report No. 218, Max-Planck-Institut für Meteorologie, Hamburg, Germany, 90pp.
- Roeckner, E., and Coauthors, 2003: The Atmospheric General Circulation Model ECHAM5. Part I: Model Description. MPI Report 349, Max Planck Institute for Meteorology, Hamburg, Germany, 127pp.
- Royer, J. F., F. Chauvin, B. Timbal, P. Araspin, and D. Grimal, 1998: A GCM study of the impact of greenhouse gas increase on the frequency of occurrence of tropical cyclones. *Climatic Change*, **38**(3), 307–343.
- Russell, G. L., J. R. Miller, and D. Rind, 1995: A coupled atmosphere-ocean model for transient climate change studies. *Atmos.-Ocean*, **33**, 683–730.
- Ryan, B. F., I. G. Watterson, and J. L. Evans, 1992: Tropical cyclone frequencies inferred from gray's yearly genesis parameter—Validation of GCM tropical climates. *Geophys. Res. Lett.*, **19**(18), 1831–1834.
- Shibata, K., H. Yoshimura, M. Ohizumi, M. Hosaka, and M. Sugi, 1999: A simulation of troposphere, stratosphere and mesosphere with an MRI/JMA98 GCM. *Papers in Meteorology and Geophysics*, **50**, 15–53.
- Schmidt, G. A., and Coauthors, 2006: Present day atmospheric simulations using GISS ModelE: Comparison to in-situ, satellite and reanalysis data. *J. Climate*, **19**, 153–192.
- Shepherd, J., and T. Knutson, 2007: The current debate on the linkage between global warming and hurricanes. *Geography Compass*, **1**(1), 1–24.
- Smith, R. D., and P. R. Gent, 2002: Reference Manual for the Parallel Ocean Program (POP), Ocean Component of the Community Climate System Model (CCSM2.0 and 3.0). Technical Report LA-UR-02-2484, Los Alamos National Laboratory, Los Alamos, NM.
- Terray, L., S. Valcke, and A. Piacentini, 1998: OASIS 2.2 Guide and Reference Manual. Technical Report TR/CMGC/98-05, Centre Europeen de Recherche et de Formation Avancée en Calcul Scientifique, Toulouse, France.
- Uppala, S. M., and Coauthors, 2005: The ERA-40 reanalysis. *Quart. J. Roy. Meteor. Soc.*, **131**(612), 2961–3012.
- Vecchi, G. A., and B. J. Soden, 2007: Increased tropical Atlantic wind shear in model projections of global warming. *Geophys. Res. Lett.*, **34**, L08702.
- Volodin, E. M., and N. A. Diansky, 2004: El-Niño reproduction in a coupled general circulation model of atmosphere and ocean. *Russ. Meteorol. Hydrol.*, **12**, 5–14.
- Webster, P. J., G. J. Holland, J. A. Curry, and H. R. Chang, 2005: Changes in tropical cyclone number, duration, and intensity in a warming environment. *Science*, **309**(5742), 1844–1846.
- Walsh, K., and I. G. Watterson, 1997: Tropical cyclone-like vortices in a limited area model: Comparison with observed climatology. *J. Climate*, **10**(9), 2240–2259.
- Washington, W. M., and Coauthors, 2000: Parallel Climate Model (PCM) control and transient simulations. *Climate Dyn.*, **16**, 755–774.
- Watterson, I. G., J. L. Evans, and B. F. Ryan, 1995: Seasonal and interannual variability of tropical cyclogenesis: Diagnostics from large-scale fields. *J. Climate*, **8**(12), 3052–3066.
- Yukimoto, S., and Coauthors, 2001: The new Meteorological Research Institute global ocean-atmosphere coupled GCM (MRI-CGCM2)—Model climate and variability. *Papers in Meteorology and Geophysics*, **51**, 47–88.
- Yukimoto, S., and A. Noda, 2003: Improvements of the Meteorological Research Institute Global Ocean-Atmosphere Coupled GCM (MRI-GCM2) and its Climate Sensitivity. CGER's Supercomputing Activity Report, National Institute for Environmental Studies, Ibaraki, Japan.
- Zhou, B. T., and X. Cui, 2008: Hadley circulation signal in the tropical cyclone frequency over the western North Pacific. *J. Geophys. Res.*, **113**, D16107.
- Zhou, B. T., X. Cui, and P. Zhao, 2008: Relationship between the Asian-Pacific oscillation and the tropical cyclone frequency in the western North Pacific. *Science in China(D)*, **51**(3), 380–385.